

Hybrid Model for Estimating Permitted Left-Turn Saturation Flow Rate

GANG-LEN CHANG, CHIEN-YU CHEN, AND CESAR PEREZ

This study explored the integration of analytical formulations with simulation results for estimating the complex permitted saturation flow rate. The proposed hybrid model captured most tractable interactions between the permitted flow rate and the opposing flows with the widely used formulation by Drew, which serves as one of the primary explanatory variables. To further consider the complex interactions between the permitted flow rate and all other associated factors, which often are not consistent with the assumptions used in analytical derivations, this study modeled the intractable relations as multiplicative adjustment terms and estimated their parameters with log-linear regression. Such a hybrid formulation offers the flexibility to incorporate various additional critical factors on the permitted flow rate, including the variation of driving behavior, the number of opposing lanes, the progression quality, and the heavy vehicle percentage. The preliminary tests with extensive simulation experiments have shown very promising results.

The presence of left-turning vehicles at signalized intersections tends to increase accident potential, causing excessive delay and reduction of intersection capacity. In practice, traffic engineers try to optimize the system operations with a variety of left-turn treatments such as left-turn bays, exclusive left-turn lanes, and different phasing strategies (i.e., permitted, protected, and protected-permitted). Thus, appropriate procedures for evaluation of various left-turn treatments are essential.

In reviewing the literature, it was found that most existing methods for capacity analysis start with the estimation of saturation flow rate. The capacity under various conditions can thus be obtained with appropriate adjustments of the effective green time, cycle length, and other related factors. Some prominent studies in this area include: the Illinois method (1), the revised *Highway Capacity Manual* (HCM) (2–5); Canadian methods (6), the Swedish approach (7–9), and Australian Road Research Board procedures (10). Except for the methods by Machemehl et al. (11), the core concept of all methods for permitted saturation flow rate was derived from the same queueing model of Poisson arrivals and exponentially distributed headways. Some critical factors, such as the number of opposing lanes, effects of signal control at the upstream intersection, and variation in driving populations, were either excluded from the formulation or represented with adjustment factors that are incompatible with the queueing theory. This is because the inclusion of all critical factors along with realistic assumptions in the mathematical derivation will result in complex and intractable relations, given the

current progress in the queueing theory. A comprehensive review of all existing methods, including their strengths and limitations, is available elsewhere (12).

Hence, despite the increasing attention to improving left-turn analysis, existing methods, especially for permitted saturation flow rate, retain the following critical issues:

- Trading theoretical rigor for model tractability, such as using simplified assumptions or ignoring some vital elements, in deriving a convenient analytical solution;
- Representing the complex population using limited sample field observations, such as fitting an empirical model from selected location data without reliable parameter stability; and
- Demanding very extensive field data, such as directly applying a simulation program for capacity estimation.

One of the promising alternatives to prevent the aforementioned difficulties is to develop statistical models from a well-calibrated simulation program. Conceivably, such models may not be as appealing as analytical formulations in terms of their mathematical elegance. However, they are capable of realistically incorporating related critical factors and their complex interactions through the results of simulation experiments. The stochastic nature of traffic systems, as well as the impact of various driver patterns on the resulting saturation flow rate, can also be explored with the proper design of simulation experiments. Therefore, using simulation results supplemented by field data for key parameters appears to be one of the most efficient methods.

Despite the flexibility of using statistical models from simulation results, it should be noted that the best set of parameters for a given set of observations does not necessarily reflect the actual interactions between traffic flow variables and all related factors, especially with the commonly used linear regression. Hence, the use of a hybrid model that will capture all complex relations as much as possible with analytical formulations is proposed, and then those intractable impacts from other related factors will be modeled with statistical methods such as regression. The advantages of such a method are: (a) the statistical model is nonlinear in nature but allows the performance of the estimation with the simple linear method; and (b) the method can include analytical results from some well-recognized studies in the literature that provide not only a better fit to the data but also an explainable relation from the operational perspective. There are two reasons to explore the use of a hybrid approach for permitted saturation flow rate: the costs of collecting sufficient data to calibrate the model are prohibitive, and the complex interactions between permitted flow rate and all affecting factors are not analytically tractable.

G.-L. Chang and C.-Y. Chen, Department of Civil Engineering, University of Maryland at College Park, College Park, Md. 20742. C. Perez, FHWA, Turner-Fairbank Highway Research Center, ITS Division, 6300 Georgetown Pike, McLean, Va. 22101.

FACTORS AFFECTING PERMITTED SATURATION FLOW RATE

Following the saturation flow definition in HCM (2), we define the permitted left-turn saturation flow rate on an exclusive lane as follows:

Permitted left-turn saturation flow rate for an exclusive lane: the maximum number of vehicles per hour that can filter through the given opposing flows, assuming that the permitted green phase is always available to the approach and the conflicting opposing traffic.

Because left-turn vehicles are impeded by the opposing traffic under a permitted phase, the total left-turn flows are the results of sequential gap evaluations. More specifically, because of the presence of conflicting traffic, a left-turning driver has to wait for an acceptable gap to exercise a left-turn maneuver. To obtain the permitted left-turn saturation flow rate, the traffic condition must consistently have (a) some level of opposing traffic; (b) at least one queued vehicle waiting for an acceptable left-turn gap in the exclusive left-turn lane; and (c) a stochastic gap-acceptance process. To collect such data, the time period of interest should begin when all of the opposing queue have been discharged and stop when the signal changes to an amber phase.

With the above definition, factors affecting the permitted left-turn saturation flow rate include the opposing flow rate, the pattern or distribution of the opposing gaps, the gap-acceptance behavior, and the geometric conditions of the target intersection. In addition, given the same level of opposing flows, the distribution of the opposing gaps may vary dramatically depending on the signal coordination between neighboring intersections.

Critical factors associated with the permitted left-turn saturation flow rate include:

- Opposing flow rate,
- Number of opposing lanes,
- Length of opposing lanes (i.e., the distance from the target intersection to its downstream intersection),
- Speed distribution of the opposing flows,
- Heavy-vehicle percentage of the opposing flows,
- Start-up lost time and the distributions of queue discharge headways,
- Turning radius of left-turn maneuvers,
- Heavy-vehicle percentage of left-turn flows,
- Start-up lost time and discharging headways of left-turn vehicles, and
- Signal settings at the target and its upstream intersections.

EXPERIMENTAL DESIGN

As mentioned previously, because of both the difficulty in collecting sufficient permitted operation data and the resulting cost, TRAF-NETSIM has been used in this study for generating all observations. To ensure that NETSIM can realistically simulate the traffic behavior, the following parameters were calibrated with 12 field sites from three different states (Virginia, Delaware, and Florida):

- Through discharging rate and start-up delay,
- Left-turn discharging rate and start-up delay, and
- Approximate range of a permitted gap for filtering one vehicle.

The calibration process consists of the following key steps:

1. Computation from field data of start-up delays and discharging headways,
2. Stability tests with respect to sample observations from field data,
3. Computation of average discharging headway for use in NETSIM,
4. Execution of NETSIM simulations with estimated start-up delay and average discharging headway,
5. Variance analysis with respect to start-up delay and headways generated from simulation experiments with NETSIM, and
6. Test of statistical equality between queue discharging headways generated from simulation and field observations.

A detailed discussion of the calibration process can be found in Chang (13). The results of field data analyses clearly indicate that driving behavior may vary substantially from one site to the other, and the use of a reliable simulation model to generate a wide distribution of data is essential for both understanding and modeling permitted operations.

Key Variables in Simulation Experiments

Table 1 presents the variables selected as input variables in the simulation experiments for the permitted left-turn saturation flow analyses. Notably, to keep the saturated condition on the exclusive left-turn lane, one has to provide an oversaturated flow rate to the left-turn approach.

Experimental Procedures

The experimental procedures for permitted saturation flows are summarized as follows:

- As presented in Figure 1, a signalized two-intersection standard network, instead of an isolated intersection, was used for permitted left-turn saturation flows.
- In all permitted cases, in addition to the left turns, the opposing flows were varied randomly within a preselected range.
- Based on all factors in Table 1, a variety of the experimental scenarios were constructed with random sampling strategies.
- The permitted left-turn flows were collected from the time when all opposing queued vehicles had been discharged.
- The critical left-turn gaps and start-up delay, as well as discharging headways, are assumed to be normally distributed among the driving population (e.g., 10 types of drivers).
- Each sample scenario was simulated for five replications with different random number seeds. The variance of the first five replications was used to determine if any additional replication was needed.

MODEL ESTIMATION AND TESTING

The core concept of the model development is to take advantage of existing analytical studies and then supplement such results with some adjustment factors to account for other critical factors. The reason is that, although analytical models can capture some primary

TABLE 1 Variables Selected for Use in Simulation Experiments for Permitted Saturation Flow Rate

Independent Variable			Lower Bound	Upper Bound	Increment
h	Mean of Queue Discharge Headway	(sec)	1.6	2.6	0.2
d	Mean of Start-Up Lost Time	(sec)	2.0	4.5	0.5
t_{cr}	Critical Gap for Left-Turn Vehicles	(sec)	3.5	6.5	0.5
L_L	Length of Exclusive Left-Turn Lane	(ft)	500	4000	500
V_L	Desired Speed of Left-Turn Flows	(mph)	25	50	5
H_L	Heavy-Vehicle Percentage of Left-Turn Flows	(%)	0	30	3
N_O	Number of Opposing Through Lanes	(lane)	1	4	1
L_O	Length of Opposing Lanes	(ft)	500	4000	500
V_O	Desired Speed of Opposing Flows	(mph)	25	50	5
H_O	Heavy-Vehicle Percentage of Opposing Flows	(%)	0	30	3
P_{OL}	Left-Turning Percentage of Opposing Flows	(%)	0	20	5
P_{OR}	Right-Turning Percentage of Opposing Flows	(%)	0	20	5
C	Signal Cycle Length in Both Intersections	(sec)	60	120	10
g_T/C	Target Green Ratio to Signal Cycle Length		0.4	0.7	0.1
g_U/C	Upstream Green Ratio to Signal Cycle Length		0.4	0.7	0.1
O_U	Signal offset in Upstream Intersection	(sec)	0	C-10	10
F_U	Flow Rate from Far Upstream Entry Node	(sec)	$100 N_O$	$0.8 Q$	100
Dependent Variable			Relationship		
g_T	Signal Green Time in Target Intersection	(sec)	$g_T = (g_T/C) C$		
r_T	Signal Red Time in Target Intersection	(sec)	$r_T = C - g_T$		
g_U	Signal Green Time in Upstream Intersection	(sec)	$g_U = (g_U/C) C$		
r_U	Signal Red Time in Upstream Intersection	(sec)	$r_U = C - g_U$		
P_{OT}	Through Percentage of Opposing Flows	(%)	$P_{OT} = 100 - P_{OL} - P_{OR}$		

Note: 1. $Q = \min(Q_U, Q_T) =$ estimated capacity of the arterial system by comparing the estimations of upstream and target intersections' capacities, where $Q_U = N_O (g_U / h) (3600 / C)$ and $Q_T = N_O (g_T / h) (3600 / C) / (P_{OT} / 100) - 200$.

2. The values of g_T and g_U should satisfy the additional requirement: $-20 \leq g_T - g_U \leq 20$.

interactions between key system factors, they are not capable of realistically representing the stochastic variations of driving behavior. For instance, the acceptable gap size of a permitted left-turn is a variable that may distribute within a wide range of a given driving population and vary with location. Drew's model (14), a special case of Tanner's formulation (15), has been selected as the principal term for use in regression analyses.

Drew's analytical model for the permitted left-turn saturation flow rate is based on the following assumptions:

- Opposing traffic is an uninterrupted flow, following a Poisson process;
- There is a continuous left-turn queue; and
- There are $(i + 1)$ left-turn vehicles that can go through a gap, if the size of the gap is t and $t_{cr} + i \cdot h \leq t \leq t_{cr} + (i + 1) \cdot h$.

Grounded on the above assumptions, an analytical solution for permitted left-turn saturation flow was given by the following equations:

$$S = F_{OT} \cdot \sum_{i=0}^{\infty} (i + 1) \cdot \Pr [t_{cr} + i \cdot h \leq t \leq t_{cr} + (i + 1) \cdot h] \quad (1)$$

and thus

$$S = F_{OT} \cdot \frac{\exp[-t_{cr} \cdot (F_{OT}/3600)]}{1 - \exp[-h \cdot (F_{OT}/3600)]} \quad (2)$$

where

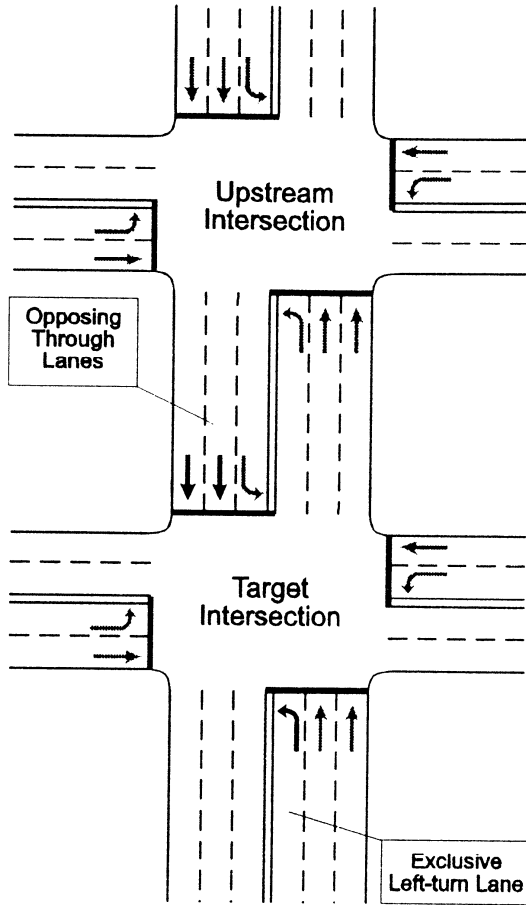
$S =$ analytical estimation of permitted left-turn saturation flow rate under F_{OT} opposing flow level (vph),

$F_{OT} =$ total flow rate of opposing through movements (vph),

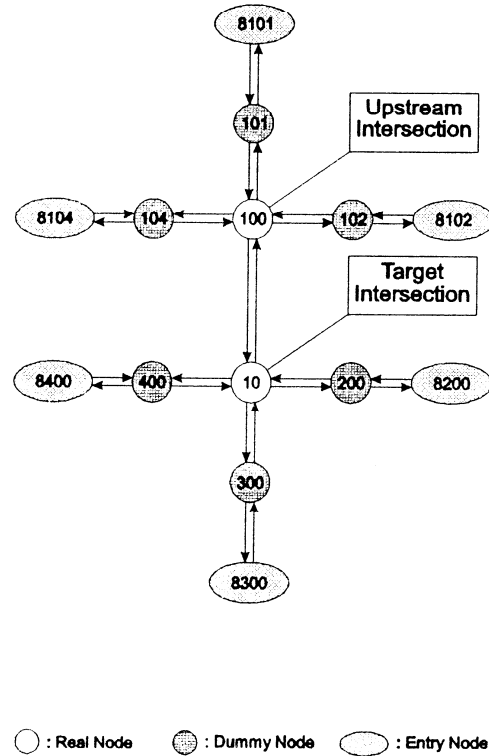
$t_{cr} =$ critical gap for left-turn vehicles (sec), and

$h =$ mean of queue discharge headways (sec).

In this study, t_{cr} and h are set to 5.0 and 2.0 sec, respectively, in Equation 2 to represent the base case. This is because TRAF-NETSIM uses 5.0 sec as its default value for critical left-turn gap,



A. Two-Intersection Network



B. Link-Node Diagram for NETSIM

FIGURE 1 Example of network used in simulation experiments for permitted left-turn saturation flow rate.

and the results of some field surveys indicate that the average queue discharge headway is around 2.0 sec. However, the variations caused by different critical gaps and discharging headways have been considered in the model with simulated data.

In addition to the above principal component, we have introduced a variable (P) to indicate the platoon arrival time in reference to the beginning of the red phase at the target intersection. As illustrated in Figure 2, P can be expressed:

$$P = \frac{\text{mod}[(T + O_U), C] - g_T}{C} \quad (3)$$

where

P = indicator of signal progression,

$T = \frac{L_o}{V_a \cdot (5280/3600)}$ = estimated link travel time (sec),

V_a = average flow speed,

L_o = length of opposing lanes (ft),

V_o = desired free flow speed or speed limit of opposing flows (mi/hr),

O_U = signal offset between target and upstream intersections (sec),

C = signal cycle length at both intersections (sec), and

g_T = signal green time at target intersection (sec).

T represents the travel time of a platoon from upstream to the target intersections. Because of the signal offset at the upstream intersection (O_U), the platoon's actual arrival time should be $T + O_U$ at the target intersection. Furthermore, the arrival time is $\text{mod}(T + O_U, C)$ sec after the beginning of a given cycle during which the platoon will arrive and, hence, is $\text{mod}(T + O_U, C) - g_T$ sec after [or $g_T - \text{mod}(T + O_U, C)$ sec before] the start of the red signal time in that cycle. Finally, to eliminate the scalar effect of signal cycle length, the above term is divided by the signal cycle length C , as shown in Equation 3. The P value lies within the range $-g_T/C \leq P < 1 - g_T/C$; thus, a higher P value implies better coordination between signals and results in a shorter queue length and a greater permitted left-

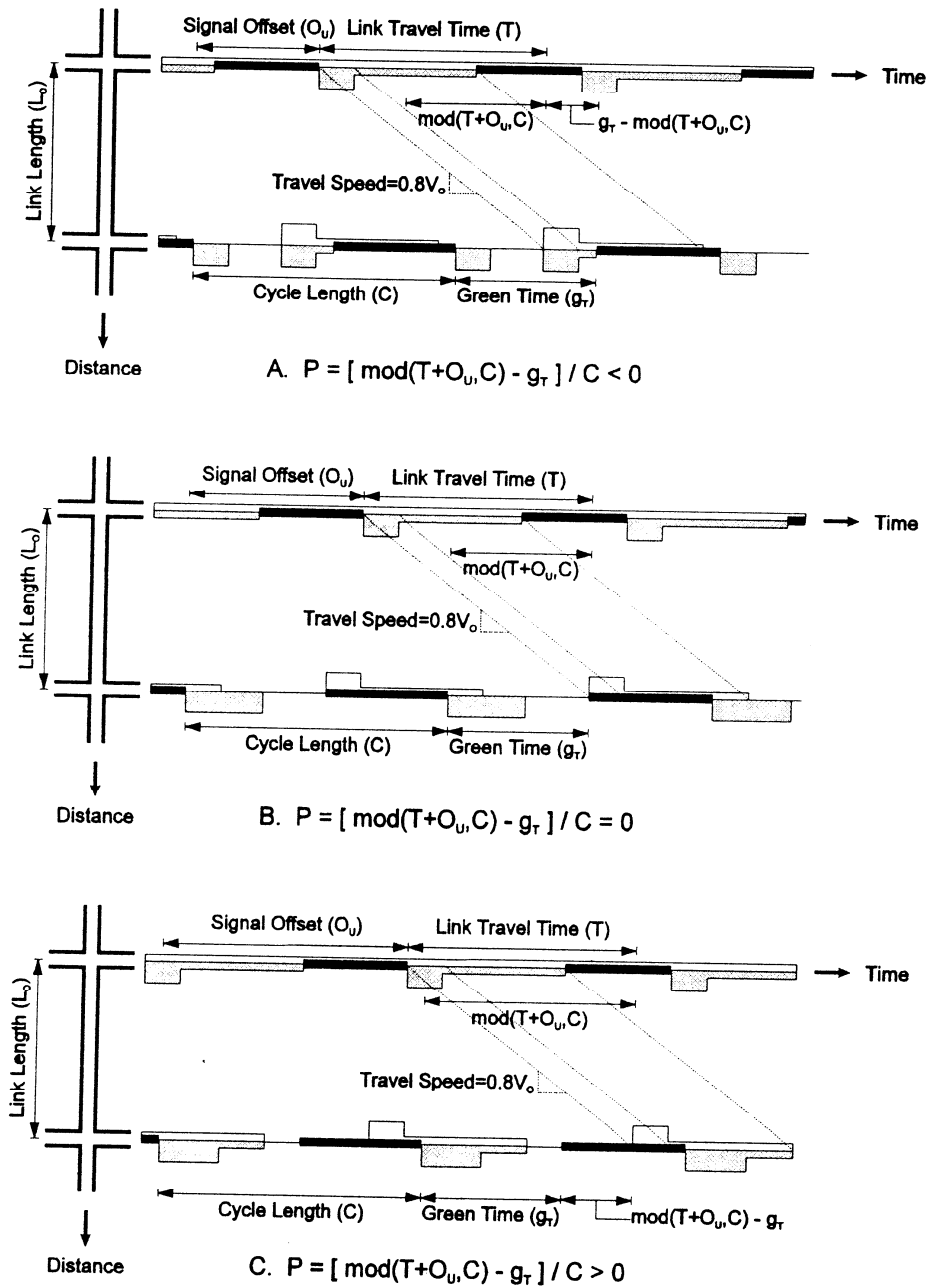


FIGURE 2 Illustration of variable P (indicator of signal progression).

turn saturation flow rate. In other words, one can expect a positive correlation between P and S_{PM} .

To eliminate all highly correlated factors, a correlation analysis, with 300 observations was conducted for all variables involved in the simulation experiments. Table 2 summarizes the results of those highly correlated with the permitted left-turn saturation flow rate (S_{PM}), including:

- Average queue discharge headway (h),
- Critical gap for left-turn vehicles (t_{cr}),
- Heavy-vehicle percentage of left-turn flows (H_L).

- Number of opposing lanes (N_o),
- Total opposing through flow rate (F_{OT}),
- Opposing right-turn flow rate (F_{OR}),
- Analytical estimation of permitted left-turn saturation flow rate (S), and
- Indicator for the quality of signal progression (P).

As expected, all opposing-flow-related variables (F_{OT} , F_{OR} and S) are highly correlated with S_{PM} . Because F_{OR} has a high correlation with S , it was not selected in the final model, and the inclusion of the total opposing through flows has been shown to be sufficient. This

TABLE 2 Correlation Coefficients of Key Variables for Permitted Left-Turn Saturation Flow Rate

Pearson Correlation Coefficients / Prob > R under Ho: Rho=0 / N = 300									
	SPM	H	TCR	HL	NO	FOT	FOR	S	P
SPM	1.00000 0.0	-0.17439 0.0024	-0.26945 0.0001	-0.15066 0.0090	-0.36708 0.0001	-0.80733 0.0001	-0.44564 0.0001	0.88598 0.0001	0.29728 0.0001
H	-0.17439 0.0024	1.00000 0.0	-0.10885 0.0597	0.02048 0.7238	0.09051 0.1177	-0.01131 0.8454	-0.03665 0.5271	-0.00682 0.9064	0.07923 0.1711
TCR	-0.26945 0.0001	-0.10885 0.0597	1.00000 0.0	0.04080 0.4814	0.03281 0.5713	0.02741 0.6363	-0.00699 0.9040	-0.05624 0.3316	-0.10818 0.0613
HL	-0.15066 0.0090	0.02048 0.7238	0.04080 0.4814	1.00000 0.0	0.00456 0.9373	0.02168 0.7084	0.08237 0.1547	-0.04809 0.4066	-0.09933 0.0859
NO	-0.36708 0.0001	0.09051 0.1177	0.03281 0.5713	0.00456 0.9373	1.00000 0.0	0.44647 0.0001	0.31087 0.0001	-0.41374 0.0001	-0.09754 0.0917
FOT	-0.80733 0.0001	-0.01131 0.8454	0.02741 0.6363	0.02168 0.7084	0.44647 0.0001	1.00000 0.0	0.48679 0.0001	-0.85620 0.0001	-0.12952 0.0249
FOR	-0.44564 0.0001	-0.03665 0.5271	-0.00699 0.9040	0.08237 0.1547	0.31087 0.0001	0.48679 0.0001	1.00000 0.0	-0.51493 0.0001	-0.14782 0.0104
S	0.88598 0.0001	-0.00682 0.9064	-0.05624 0.3316	-0.04809 0.4066	-0.41374 0.0001	-0.85620 0.0001	-0.51493 0.0001	1.00000 0.0	0.22996 0.0001
P	0.29728 0.0001	0.07923 0.1711	-0.10818 0.0613	-0.09933 0.0859	-0.09754 0.0917	-0.12952 0.0249	-0.14782 0.0104	0.22996 0.0001	1.00000 0.0

is mainly because of the design of scenarios in which only one left-turn lane was considered in all cases.

The estimation results of a preliminary linear model with all the above key factors are shown below:

$$S_{PM} = 959 + 0.49 \cdot S - 88 \cdot (t_{cr} - 5.0) - 264 \cdot (h - 2.0) - 64 \cdot N_o - 0.37 \cdot \frac{F_{OT}}{N_o} + 139 \cdot P - 3.77 \cdot H_L$$

R^2 value = 0.91 Number of observations = 300 (4)

Coefficient	t-value
959	14.0
0.49	12.9
88	-13.1
264	12.6
64	-6.4
0.37	-9.5
139	6.1
3.77	-5.4

In Equation 4,

S_{PM} = permitted left-turn saturation flow rate (vph),

$$S = F_{OT} \cdot \frac{\exp[-5.0] \cdot (F_{OT}/3600)}{1 - \exp[-2.0 \cdot (F_{OT}/3600)]} = \text{analytical estimation of the permitted left-turn saturation flow rate under } F_{OT} \text{ opposing flow level (vph),}$$

F_{OT} = opposing through flow level (lane),

N_o = number of opposing through lanes (lane),

$$P = \frac{\text{mod}[(T + O_U), C] - g_T}{C} = \text{indicator of signal progression,}$$

H_L = heavy-vehicle percentage of left-turn flows, and

$$T = \frac{L_o}{0.8 \cdot V_o \cdot (5280/3600)} = \text{estimated link travel time (sec).}$$

Basically, the R^2 value and the t -value for each parameter appear to be satisfactory, considering the large number of factors involved. In addition, the sign of each parameter is also consistent with the observed traffic flow relations. The implication is that the permitted left-turn saturation flow rate (S_{PM}) will increase when either factor S or P increases and will decrease with an increase in the average queue discharge headway (h), the critical left-turn gap (t_{cr}), the heavy-vehicle percentage (H_L), the number of opposing lanes (N_o), and the opposing through flow rate (F_{OT}).

It is notable that the terms $h - 2.0$ and $t_{cr} - 5.0$ are designed to reflect various types of driving behavior, where the h and t_{cr} may not equal 2.0 and 5.0 sec, respectively. In addition to the total opposing through flow rate (F_{OT}), the model also contains the term (F_{OT}/N_o), the opposing through flow rate per lane, to capture the compound effect.

Figure 3 presents the residual distribution that exhibits its consistency with some basic regression assumptions, such as a zero mean and constant variance. To further consider the convenience of applications, such a complex relation has been captured with a multiplicative form so that the effect of each individual variable can be represented as an adjustment factor such as those used in the HCM.

Thus, for convenience of applications, a revised log-linear model was developed and is presented as follows:

$$\ln(S_{PM}) = 5.19 + 0.32 \cdot \ln(S) - 0.6 \cdot \ln\left(\frac{t_{cr}}{5.0}\right) - 0.69 \cdot \ln\left(\frac{h}{2.0}\right) - 0.0005 \cdot \left(\frac{F_{OT}}{N_o}\right) - 0.08 \cdot N_o + 0.32 \cdot P - 0.57 \cdot \ln(1 + 0.01 \cdot H_L)$$

R^2 value = 0.89 Number of observations = 300

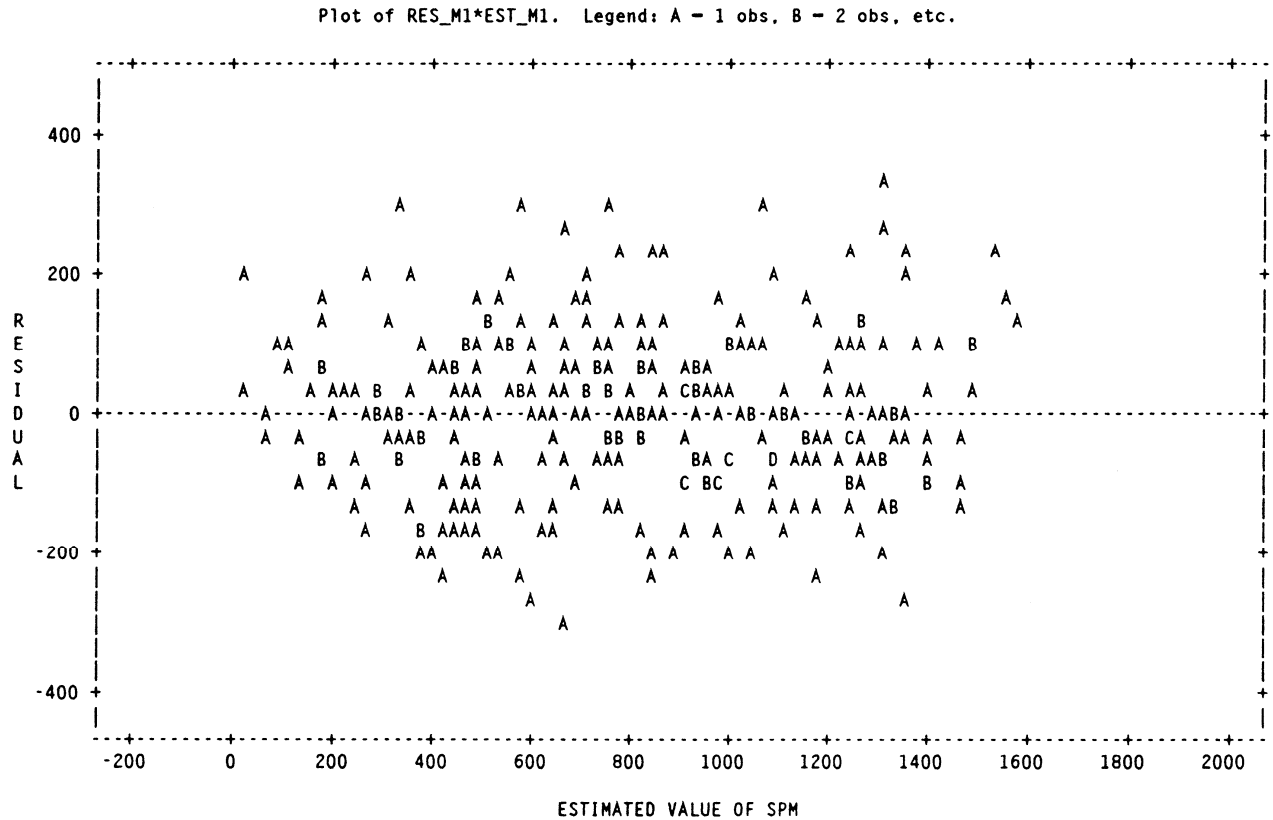


FIGURE 3 Plot of residuals versus estimated values for permitted saturation flows from preliminary (linear) model.

Coefficient	t-value
5.19	20.5
0.32	12.1
0.63	-9.6
0.69	-8.0
0.0005	-6.3
0.08	-3.7
0.32	7.2
0.57	-3.6

which is exactly equivalent to the following multiplicative form:

$$S_{PM} = 180 \cdot (S)^{0.32} \cdot \left(\frac{t_{cr}}{5.0}\right)^{-0.63} \cdot \left(\frac{h}{2.0}\right)^{-0.69} \cdot \left[\exp\left(\frac{F_{OR}}{N_o}\right)\right]^{-0.0005} \times [\exp(N_o)]^{-0.08} \cdot [\exp(P)]^{0.32} \cdot (1 + 0.01 \cdot H_L)^{-0.57} \quad (6)$$

or

$$S_{PM} = 180 \cdot (S)^{0.32} \cdot \left(\frac{t_{cr}}{5.0}\right)^{-0.63} \cdot \left(\frac{h}{2.0}\right)^{-0.69} \cdot (0.9995)^{F_{OR}/N_o} \cdot (0.9223)^{N_o} \times (137)^P \cdot (1 + 0.01 \cdot H_L)^{-0.57} \quad (7)$$

Note that to best fit the data in Equation 5, some of the regressors, (F_{OR}/N_o), N_o , and P , have remained in their original forms. Equation 5 can be transformed into Equation 6 or 7 by taking the exponential transformation on both sides.

As expected, the sign for each parameter is consistent with the preliminary linear model. Both the overall R^2 value and the t -value for each parameter have shown the promise of the proposed model structure. Figure 4 further presents the residual distribution of

the revised multiplicative model that also shows an acceptable pattern.

To test the performance of the revised model, an additional 50 simulation cases were executed. Figure 5 illustrates the frequency distribution of the estimated errors on the basis of the revised model (Equation 7). Most of the estimated values are within a reasonable range of their observed values.

Stability Test

Because stability is one of the essential properties for a statistical model, the Chow test (16) was used to evaluate the revised log-linear model for permitted left-turn saturation flow rate. Table 3 summarizes the statistics and the testing results of the revised log-linear model. Because the statistic F^* of the model is obviously less than the critical value $F_{0.05,1,12}$, it can be concluded that both the model structure and parameters have no significant difference between the first and the second data subsets; that is, the estimated parameters and relations are independent of the selected sample size.

Performance Evaluation

Although in conducting this study, permitted data have been collected from several field sites, the results are not sufficient for use in model evaluation. This is because all such sites having heavy left-turn flows have been changed to either protected or protected-permitted control. All those currently under permitted control have the flow rate far under the saturation level. Hence, we have selected

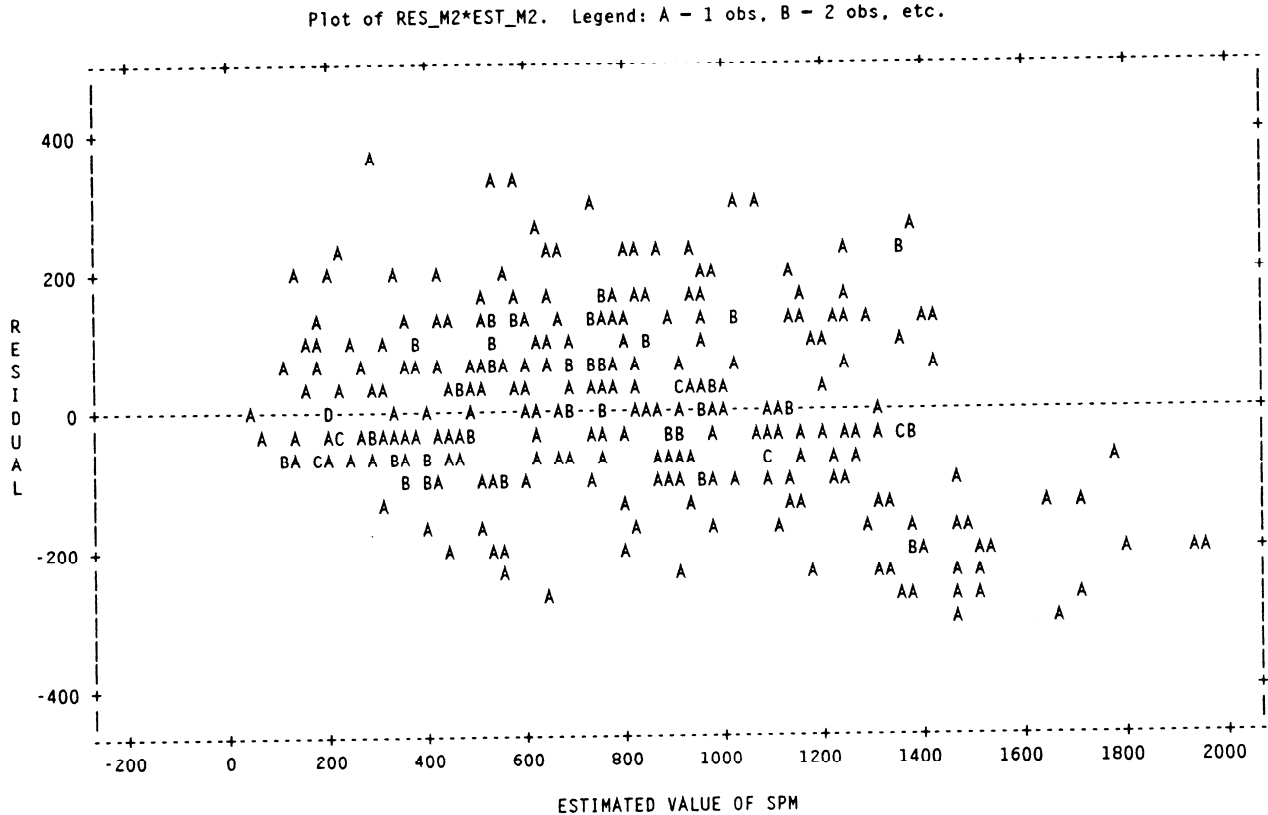


FIGURE 4 Plot of residuals versus estimated values for permitted saturation flows from revised (log-linear) model.

the simulated scenarios, which cover a wide range of traffic conditions, for model comparison and performance evaluation.

Fifty more cases were generated using the random sampling strategy for model performance evaluation described earlier. The comparison results, based on the proposed model, the procedures in HCM, and the permitted flow rate collected from the simulation, are presented in Figure 6. As is evidenced in the graphical interrelations, the proposed model has yielded the permitted flow rate quite consistent with results from the simulation (TRAF-NETSIM). In contrast, the procedures from HCM have consistently underestimated the permitted flow rate. This is because the procedures from HCM remain grounded on the same assumption of Poisson arrival patterns used in Drew's model (the first term in our proposed model) and in most existing analytical formulations.

The research team has fully recognized the potential discrepancy between the simulated and field observation results. However, because of the extreme difficulty in having reliable field data and adequate samples, the use of a well-recognized simulation program with carefully calibrated parameters is certainly one of the acceptable alternatives. The fact that the proposed model has performed reasonably well under various simulated systems is thus encouraging and deserving of further development along the same line.

CONCLUSIONS

The left-turn saturation flow rate is one of the most critical factors for estimating the capacity of left-turn approaches and for evaluating the performance of left-turn operational alternatives. Given a

reliable estimate of saturation flow rate, one can easily compute the resulting capacity under various signal control strategies. This study has presented a hybrid model for estimating the left-turn saturation flows under permitted phasing for an exclusive lane. Such a model, grounded on field data and extensive simulation results, has circumvented most difficulties encountered in existing HCM procedures and allows one to take into account all critical factors as well as behavioral differences in various driving populations. The findings and conclusions of this study are summarized:

- The proposed permitted left-turn saturation flow model reliably captures the impacts of various critical factors, including the critical left-turn gap, the queue discharge headway, the number of opposing through lanes, or the opposing through flow per lane. In addition, the permitted left-turn saturation flow rate increases with the analytical results for permitted left-turn saturation flows and the indicator of signal progression.
- Because of the embedded driving behavior-related factors, such as queue discharge headway and critical left-turn gap, the proposed model has the flexibility to reflect various types of the driving population.
- Although the developed model does not have the mathematical elegance of analytical formulations, it is capable of realistically incorporating all associated factors and their collective impacts in real-world operations.
- On the basis of the results of the Chow stability test, the proposed model shows that both the model structure and the parameters are quite stable and independent of sample size.

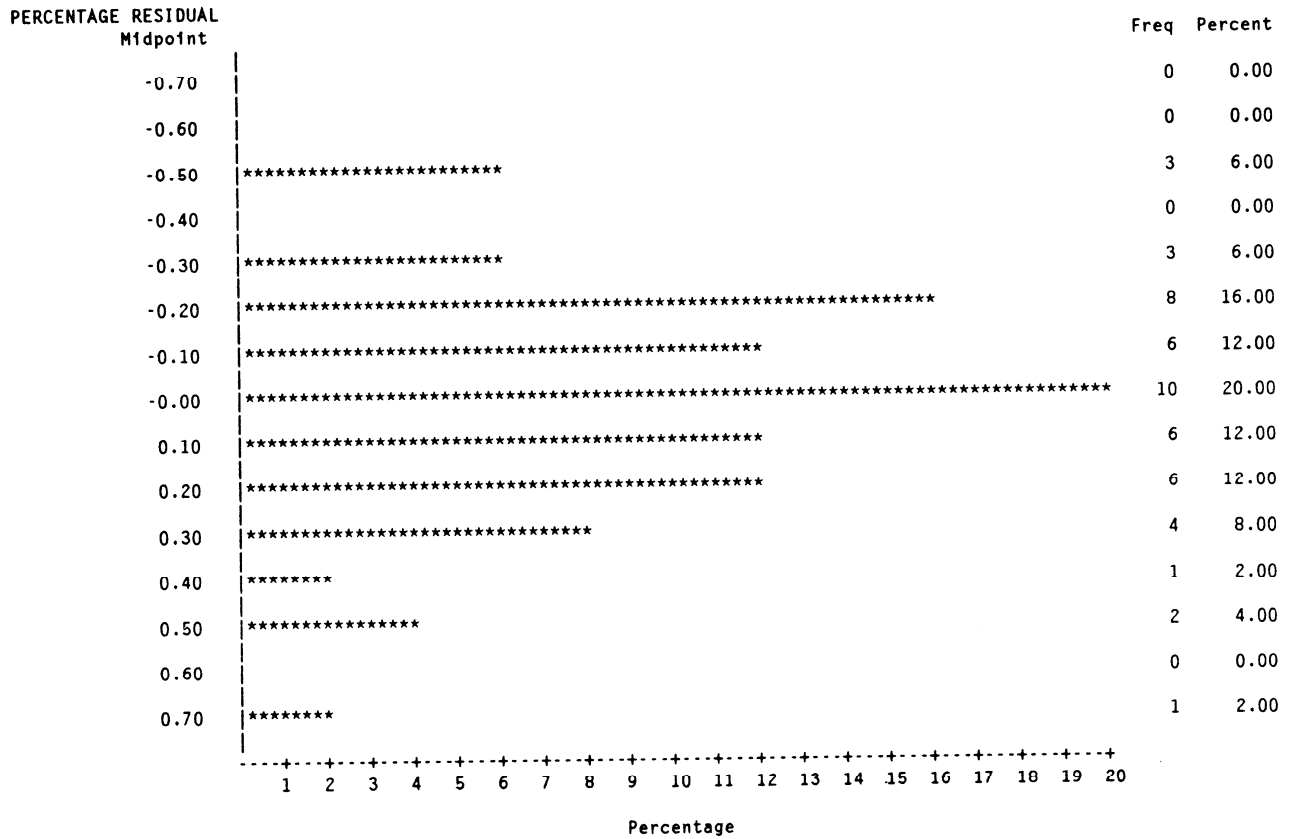


FIGURE 5 Percentage error distribution of estimated values for permitted left-turn saturation flows from revised (multiplicative) model.

TABLE 3 Summary of Revised (Log-Linear) Models and Test Results for Permitted Left-Turn Saturation Flow Rate

Basic Statistic	Pooled Data		First Subset		Second Subset	
No. of Observations	300		150		150	
R ² Value	0.8864		0.9182		0.8478	
Model SS (df)	125.9004	(7)	74.5966	(7)	50.9138	(7)
Error SS (df)	16.1283	(292)	6.6468	(142)	9.1380	(142)
Total SS (df)	142.0287	(299)	81.2434	(149)	60.0518	(149)
Variable	Parameter (t-Value)		Parameter (t-Value)		Parameter (t-Value)	
Intercept	5.1914	(20.53)	4.9434	(16.34)	5.5604	(12.70)
ln(S)	0.3221	(12.12)	0.3500	(11.05)	0.2806	(6.06)
ln(t ₀₁ /5.0)	-0.6284	(-9.61)	-0.5637	(-6.45)	-0.6655	(-6.70)
ln(h/2.0)	-0.6871	(-8.03)	-0.7809	(-7.07)	-0.6017	(-4.51)
F ₀₁ /N ₀	-0.0005	(-6.27)	-0.0005	(-4.92)	-0.0006	(-4.10)
N ₀	-0.0809	(-3.65)	-0.0611	(-2.18)	-0.1059	(-2.96)
P	0.3150	(7.17)	0.3622	(6.37)	0.2926	(4.19)
ln(1+0.01H _L)	-0.5717	(-3.60)	-0.5047	(-2.33)	-0.6623	(-2.78)
Testing Statistic	Chow Test -- Testing the stability of model parameters					
F [*] Statistic	0.7728					
F _{.05,v1,v2}	1.9711					
H ₀ : b ₁ = b ₂	Accept					

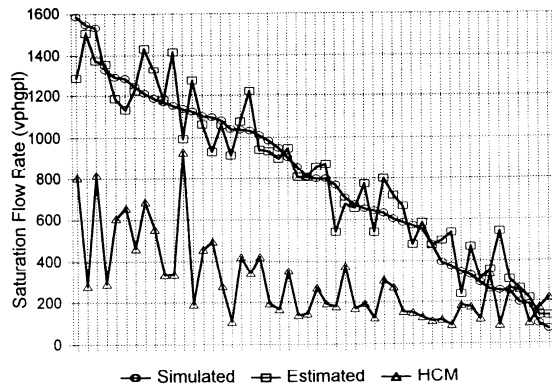


FIGURE 6 Comparison of performance between HCM procedures and proposed model.

- Use of simulation methods not only circumvents the need for extensive field data, which often results in prohibitive costs, but also effectively yields some vital information that cannot be accurately measured from field observations.

- To further understand the characteristics of left-turn saturation flows, it will be necessary to investigate (a) the protected left-turn saturation flow models for exclusive double and triple left-turn lanes, (b) the left-turn flow filtering rate during the transition period of the protected-permitted and permitted-protected signal phasings, and (c) the effects of U-turning vehicles on the left-turn saturation flows.

- To accomplish the left-turn capacity analysis, at least two more factors should be taken into account: a reliable queuing model for estimating the average queue length on the opposing through lanes and for computing the effective green time for left-turning vehicles, and the effect of various bay lengths on the left-turn capacity under both protected and permitted phasings.

ACKNOWLEDGEMENT

This project was supported by FHWA, U.S. Department of Transportation.

REFERENCES

1. Rouphail, N. M. Magnuson, and V. Sisiopiku. *Validation of 1985 HCM Procedures for Capacity and LOS of Left-Turn Lanes in Illinois*. Report FHWA/IL/RC-012. FHWA, U.S. Department of Transportation, 1991.
2. *Special Report 209: Highway Capacity Manual*, 3rd ed. TRB, National Research Council, Washington, D.C., 1985.
3. Roess, R. P. Development of Analysis Procedures for Signalized Intersections in the 1985 *Highway Capacity Manual*. In *Transportation Research Record 1112*, TRB, National Research Council, Washington, D.C., 1987, pp. 10–16.
4. Roess, R. P., V. N. Papayannoulis, J. M. Ulerio, and H. S. Levinson. *Levels of Service in Shared Permissive Left-Turn Lane Groups of Signalized Intersection*. Report FHWA-RD-89-228. FHWA, U.S. Department of Transportation, 1989.
5. Roess, R. P., J. M. Ulerio, and V. N. Papayannoulis. Modeling the Left-Turn Adjustment Factor for Permitted Left Turns Made from Shared Lane Groups. In *Transportation Research Record 1287*, TRB, National Research Council, Washington, D.C., 1990, pp. 138–150.
6. Teply, S. Canadian Capacity Guild for Signalized Intersections: An Overview. *Proc., 9th Annual Conference*. ITE, District 7, Canada, 1984.
7. Hansson, A., and T. Bergh. A New Swedish Capacity Manual/CAPCAL 2. Presented at 14th Conference of the Australian Road Research Board, 1988.
8. Peterson, B. E., A. Hansson, and K. L. Bång. Swedish Capacity Manual. In *Transportation Research Record 667*, TRB, National Research Council, Washington, D.C., 1978, pp. 1–28.
9. *Swedish Highway Capacity Manual*. National Swedish Road Administration, 1977.
10. Akcelik, R. *Traffic Signal: Capacity and Timing Analysis*. Reprint of Research Report ARR 123, 1981. Australian Road Research Board, Nunawading, 1989.
11. Machemehl, R. B., H. J. Lin, C. E. Lee, and R. Herman. *Guidelines for Use of Left-Turn Lanes and Signal Phases*. Research Report 258-1. Center for Transportation Research, University of Texas at Austin, 1984.
12. Chang, G. L., L. Zhuang, and E. V. Cater. *Task A: Literature Review—A Study to Develop Revised Planning Methodology for Signalized Intersection and Operational Analysis of Exclusive Left-Turn Lanes*. Report DTFH 61-92-00109. FHWA, U.S. Department of Transportation, 1993.
13. Chang, G. L. *Analyses of Left-Turn Operations—Part III: Field Data Collection and Summary*. Report DTFH 61-92-00109. FHWA, U.S. Department of Transportation, 1995.
14. Drew, D. R. *Traffic Flow Theory and Control*. McGraw-Hill, New York, 1968.
15. Tanner, J. C. The Capacity of an Unsignalized Intersection. *Biometrika* 54, 1967, pp. 657–658.
16. Chow, C. C. Tests of Equality Between Sets of Coefficients in Two Linear Regressions. *Econometrica*, Vol. 28, 1960, pp. 591–605.